Cabling Constraints in PV Array Architecture: Design, Mathematical Model and Cost Analysis

FAHAD USMAN KHAN[ID][1], **ALI FAISAL MURTAZA**[ID][1], **(Member, IEEE),**
HADEED AHMED SHER[2], **(Senior Member, IEEE),**
KAMAL AL-HADDAD[ID][3], **(Life Fellow, IEEE),**
AND FAISAL MUSTAFA[4]

[1]Faculty of Engineering, University of Central Punjab, Lahore 54000, Pakistan
[2]Faculty of Electrical Engineering, Ghulam Ishaq Khan Institute of Engineering Sciences and Technology, Topi 23460, Pakistan
[3]École de Technologie Supérieure (ÉTS), University of Quebec, Montreal, QC H3C 1K3, Canada
[4]Faculty of Management Sciences, University of Central Punjab, Lahore 54000, Pakistan

Corresponding author: Fahad Usman Khan (fahadusman44@gmail.com)

ABSTRACT In this article, cabling constraints of different photovoltaic (PV) configurations is addressed in three steps: 1) a cable selection criterion is developed in accordance with metric system defined by American Wire Gauge (AWG); 2) a mathematical model is designed, which estimates the cable length for any array size; and 3) cost functions are devised owing to estimate the cables capital expenditure. The aforementioned steps are developed for Series (S), Parallel (P), Series-Parallel (SP), Total-cross-tied (TCT), Bridge-Link (BL) and Honey-Comb (HC). A comprehensive mathematical model is developed for each of the above mentioned architectures in the context of cabling cost versus energy payback time. This cost analysis provides a clear snapshot to the designers of PV plant about the capital investments of cabling system of specific architecture and its potential energy payback time. At the end, a design example for each configuration is presented against an array size of 10×2 PV panels.

INDEX TERMS Series-parallel (SP), bridge-linked (BL), honey-comb (HC), total cross tied (TCT), cabling constraints, cost analysis.

NOMENCLATURE

W_M	Width of module
L_M	Length of module
B_L	Base Length
R_{SP}	Distance of row spacing
I_{SC}	Short Circuit Current of PV Module
L_{M-M}	Cable length between two consecutive modules with-in a string
$L_{Str-Str}$	Cable length between two consecutive strings
$L_{Cab(M\_M)}$	Total cable length for module-to-module
$L_{Cab(Str-Str)}$	Total cable length for string-to-string
L_{RT}	Extra round trip of cable length to reach inverter
θ_1	PV Tilt Angle
θ_2	Solar Elevation Angle
N_M	Number of Modules in a String
N_{str}	Number of Strings in an Array
N_{HC}	No of Inter Strings Connection in Honey Comb Array
I_{M_M}	Module-to-module current
$I_{Str-Str}$	String-to-string current
TCF	Temp. Correction Factor
T_H	Highest temperature of installation field
$I_{Rated(M-M)}$	Rated current module-to-module
$I_{Rated(Str-Str)}$	Rated current module-to-module
$C_{Cab(M-M)}$	Cost of cable module-to-module
$C_{Cab(Str-Str)}$	Cost of cable string-to-string
C_{Total}	Total cost of cabling

The associate editor coordinating the review of this manuscript and approving it for publication was Ahmed F. Zobaa[ID].

I. INTRODUCTION

The desire to tackle the environmental challenges and to yield sustainable energy acknowledging the fact that fossil fuel is running out have gathered the worldwide efforts. One of the favorable renewable energy resources is Photovoltaic (PV), given the abundant of solar energy source [1]. In this regard, the trend of grid-connected PV system residential scale

(of few Kilowatts) and solar PV farms scale (Megawatts) is growing rapidly. Moreover, the energy generated by PV is environment friendly, simple to experiment, and faster to implement. The efficiency and performance of PV depend on various factors but the disparities in irradiance and temperature are considered as the most influential factors on the PV systems [2]. Many reconfiguration schemes of PV array are used to harvest the maximum output power under these influential factors. Mostly used configurations are: Series (S), Parallel (P), Series-Parallel (SP), Total-cross-tied (TCT), Bridge-Link (BL) and Honey-Comb (HC).

In [2] the comparative study of PV array of size 3×3 is done between SP and TCT architectures using MATLAB/ Simulink systems. The results from the literature show that the TCT architecture is more cable of generating larger output power compared to SP under the effect of shading. In [2], it is clear that magic square view can help the TCT architecture to harvest more power from solar energy when compared the TCT with SDK schemes.

TCT is considered the most optimal architecture used for symmetrical array size trailed by HC [3]. Difference in the power between TCT and HC is about 5% for an array size 3×3 at certain value of irradiance. The comparison between these schemes is found in the literature is only based on the maximum output power under different constraints such as partial shading. The fact of initial implementation cost is entirely ignored. Similarly in [4] Sudoku is a reconfigurable method that enhances the power output of a PV array as compared to the other PV configurations [4]. The results in [4] shows that generated power of TCT and Sudoku is same, the only difference is the losses which are 3% less in Sudoku as compared to TCT. But the inter string cable requirements must be far greater as compared to any of the other PV configurations. Therefore, the percentage increment in the cost of the system will be far greater than the others. Besides the disadvantages of greater complexity and higher cost, the reduction in power loss due to this approach can be very useful for small-scale installations in urban environments having the high possibility of partial shading [4]. In [5] power enhancement when compared to TCT under partial shading is 3% to 6% but due to increased interconnections the amount of cable used is almost double resulting a definite increase in the cost.

Electrical array reconfiguration (EAR) scheme and the recommended scheme in [6] harvest the same power under different shading conditions applied on PV arrays. Most of the faults in PV system are caused by 'cable insulation failure', 'aging', 'impact damage', 'water leakage', 'insulation damage of cables due to chewing done by rodents' and accidental short circuit or arcing inside the PV combiner box caused by corrosion [7]. These facts leads to the proper selection of cable size in American wire Gauge (AWG) and insulation type to reduce the occurrence of faults and arcing at high voltage. For the cable having gauge of 1.5, 4 and 10 mm^2, the losses are inspected within the framework. The results are elaborated as: heat losses goes up to 5.7%, the unit quality

losses are nearly 3%, the losses caused by inverter are around 18% and the losses due to the partial shading can be up to 33% of the total power loss. . For the cable having gauge of 1.5, 4 and 10 mm^2, the losses are merely 1.7%, 0.6% and 0.2% respectively [8], [9].

From aforementioned literature survey, it can be deduced that quantitative analysis to determine optimal cable size and properly designing the minimum strings distance required in an array for avoiding the unwanted shading is very important in terms of system efficiency and optimized cost. Following factors are taken into account in selecting the array configuration and interconnection cable type:

1) **Cable Insulation Failure**: Most of the ground faults in PV system are caused due to the insulation failure of the cable used. If the cable is not designed to handle the current ratings or ambient temperature according to NEC standards can lead to ground fault.

2) **Arcing**: Arcing is caused mostly due to the insulation failure of the cable at the connection box leading to fire. The proper selection of cable AWG and insulation at ambient temperature for the system can reduce the occurrence of such events.

3) **Power loss Vs. System Cost**: Smaller value of the AWG of cable tend to cause more voltage drop and have less power handling capacity with less cost. On the other hand Larger AWG has an advantage of less voltage drop, larger power handling capacity but the cabling cost will increase depending upon the chosen array configuration.

4) **Partial Shading**: Partial shading and degradation are the major causes of mismatches on PV arrays which usually lead to power loss and hot spots on PV modules. TCT shows better results in terms of power loss under partial shading followed by HC when compared to the other array configurations leading to the conclusion of preferably using TCT. The implementation cost of any array configuration must also have an influential effect on its selection rather than relying only on its power output.

None of the above mentioned literature survey discusses the cost of implementation of any of the array configuration. For the past decade the main focus of the researchers were on increasing PV cell productivity under various weather conditions [9], maximum power point tracking techniques to deal with the issues like partial shading and others [10], and different design and interfacing techniques of inverter to PV arrays [11]. But the idea of the selection of an optimal (AWG/mm^2) cable for the PV system and its application is given very minimum attention in the literature. Because of I-V characteristics of PV modules, the maximum current supplied by PV to the system is always within the range of its short-circuit current. Therefore, the AWG of the cables and fuse ratings for any PV array are usually decided based on the Isc [12]. In this article we provide the proper designing of PV array and quantitative solution of finding the estimated cost for interconnections of the six static PV array
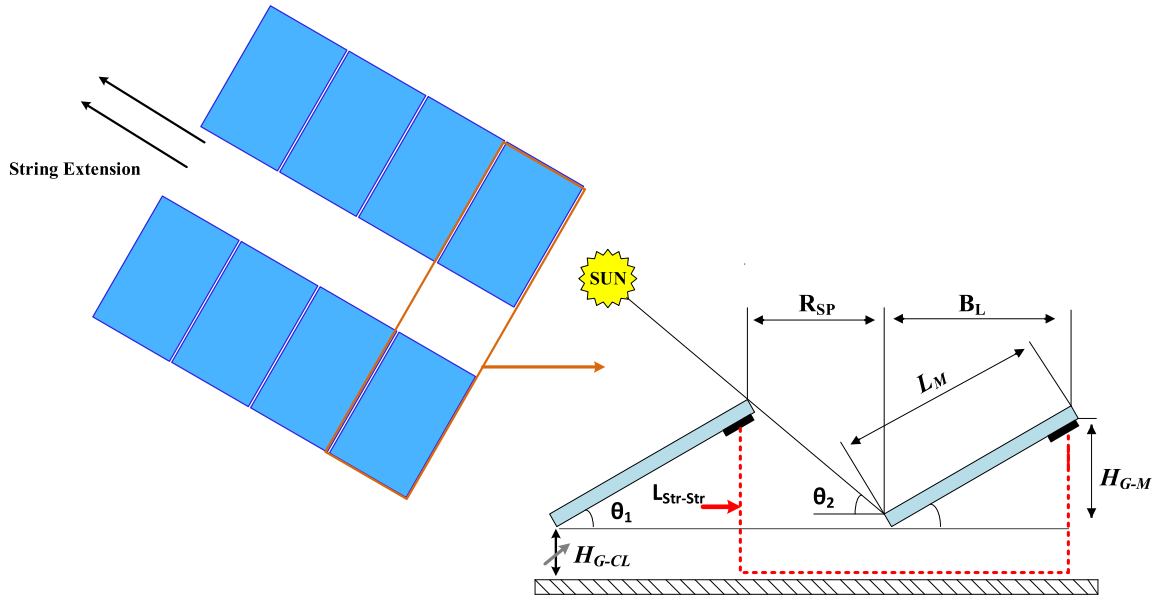
FIGURE 1. Spacing b/w strings of PV module.

configurations including proper ampacity (ampere capacity) design of cables. The Dynamic configurations are not discussed due to their complex cabling constraints and other limitations.

In summary, following contributions are made:

1. AWG selection criteria of the cable is discussed considering the value of rated current of system, allowable voltage drop and temperature of the installation location according the National Electric Code NEC) standards.
2. The design criteria to get optimal value of minimum string spacing of the array is discussed for avoiding partial shading due to adjacent strings and to utilize most of the installation site results in terms of maximum power and array size.
3. For the first time a comprehensive cost analysis is given for PV arrays existing configurations. This quantitative analysis can be applied on array of any size to get estimated cost by just knowing the module dimensions and the price of the cable used.

DC distribution with low power has the edge of safety and reliability with more flexibility over high voltage distribution systems [13]. The NEC provisions for low voltage DC systems are the proof of considering safety over efficiency by accurately analyzing the wire size after the voltage drop, system efficiency and future load requirements are taken into account [14].

II. MATHEMATICAL MODEL OF CABLE LENGTH FOR SIX INTERCONNECTION SCHEMES

In general, PV modules are ground mounted in the form of strings, where they remain static at optimum angles of tilt (θ_1), azimuth and elevation according to the site location. The appropriate row spacing between every two consecutive strings is critical and troublesome in order to avoid the shading effect. The illustration of this concept is presented in Fig 1. Here, the length of interconnection cable between two PV strings involves: 1) height between ground surface and module junction box (H_{G-M}) – by using length of module (L_M) and tilt angle (θ_1), the perpendicular (equal to height) is estimated through trigonometric relation as presented in (1), 2) distance of row spacing (R_{SP}) between two strings – by using elevation angle (θ_2) and H_{G-M}, the base (equal to row spacing) is calculated through trigonometric relation as presented in (2), 3) base length of tilted module (B_L) - by using tilt angle (θ_1) and L_M, the base length is calculated through trigonometric relation as presented in (3) and 4) ground clearance of module lower edge represented as H_{G-CL}, a variable depends on the height of pole on which P module is mounted.

$$H_{G-M} = Sin(\theta_1) \times L_M \tag{1}$$

$$R_{SP} = \frac{H_{G-M}}{Tan(\theta_2)} = \frac{Sin(\theta_1) \times L_M}{Tan(\theta_2)} \tag{2}$$

$$B_L = Cos(\theta_1) \times L_M \tag{3}$$

With the sum of (1), (2), (3) and H_{G-CL} the cable length between two consecutive strings ($L_{Str-Str}$) can be calculated from the following expression:

$$L_{Str-Str} = L_M \times \left[2Sin(\theta_1) + \frac{Sin(\theta_1)}{Tan(\theta_2)} + Cos(\theta_1) \right. $$
$$\left. + \frac{2H_{G-CL}}{L_M} \right] \tag{4}$$

For interconnection between two consecutive modules with-in a string, the cable length (L_{M-M}) can be calculated through width of module (W_M) as presented in (5), the pictorial representation of which is shown in Fig 1.

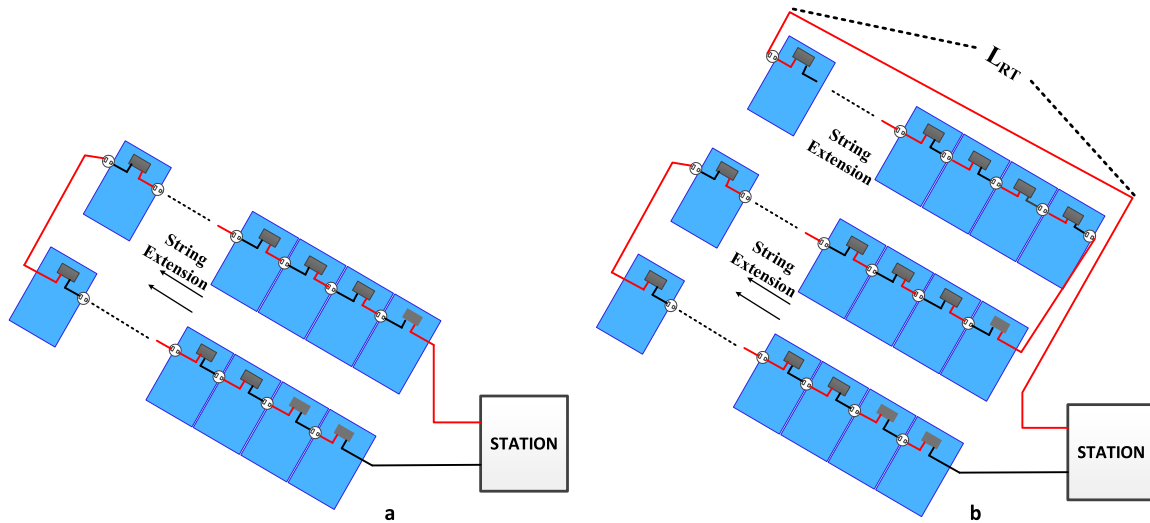$$L_{M-M} = (0.5 \times W_M) + (0.5 \times W_M) = W_M \tag{5}$$

FIGURE 2. a) Series Connection of Nm × 2 Design Array b) Series Connection of Nm × 3 Design Array with LRT.

The practical implementation of famous six schemes (S, P, SP, TCT, BL, HC) requires appropriate estimation of cable length such that capital cost of cabling can be calculated. Consequently, a generalized mathematical model is needed for each scheme, which gives a proper clue about the length of the cable and its cost. Total length of the cable will depend upon the connection scheme, size of array, and location of inverter. Location of the inverter can be fixed for any scheme and any array size. Nevertheless, the requirement of the cable will vary under different scenarios of array arrangements.

A. SERIES ARRAY

Fig. 2 reveals the PV array of series connection scheme with array size of $N_M \times N_{Str}$. Here, N_M represents the number of modules in one string, and N_{Str} represents the number of strings. For this scheme, there will be $N_{Str} - 1$ cable connections between string-to-string, and $N_{Str}(N_M - 1)$ cable connections with-in strings. By using L_{Str}-L_{Str} from (4) and L_{M-M} from (5), the generalized formula of total cable length for module-to-module and string-to-string connections are expressed in (6) & (7).

$$L_{Cab(M\_M)} = L_{M-M} \times N_{Str}(N_M - 1) \tag{6}$$

$$L_{Cab(Str-Str)} = L_{Str-Str} \times (N_{Str} - 1) + (2 \times L_{Inv} + L_{RT}) \tag{7}$$

where, L_{INV} means the length of cable required to reach inverter location in station, and 2 is incorporated as two wires i.e., +ive and –ive rail wires are involved in interfacing. L_{RT} represents the extra round trip of cable length to reach inverter if PV array has odd strings. In case of even string, it will be 0 as illustrated in Fig 2. Note that the length of L_{RT} is nearly equal to length of string, the expression of which is shown in (8)

$$L_{RT} = L_{M-M} \times N_{Str} = W_M \times N_{Str} \tag{8}$$

By putting L_{M-M} from (5), $L_{Str-Str}$ from (4) and L_{RT} from (8) in to (6) & (7), the L_{Cab_S}

$$L_{Cab(M-M)} = W_M \times N_{Str}(N_M - 1) \tag{9}$$

$$L_{Cab(Str-Str)} = L_M \times (N_{Str} - 1)\left[2Sin(\theta_1) + \frac{Sin(\theta_1)}{Tan(\theta_2)} + Cos(\theta_1) + \frac{2H_{G-CL}}{L_M}\right]$$
$$+ (2L_{Inv} + W_M \times N_{Str}) \tag{10}$$

B. PARALLEL ARRAY

The PV array with parallel interconnection scheme is presented in Fig 3. depicts the total length of cable (L_{Cab_P}) required for such a connection, where $2N_{str}(N_M - 1)$ covers the module-to-module cable for entire strings, and $2(N_{Str} - 1)$ covers the string-to-string connection for whole array. The extra cable to reach the station is $2 \times L_{Inv}$, while this connection does not require the L_{RT} as shown in Fig 3.
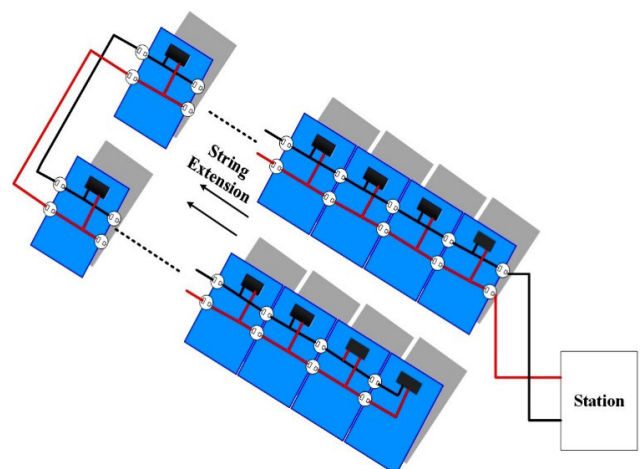

FIGURE 3. Parallel connection of Nm × 2 design array.

$$L_{Cab(M-M)} = 2N_{str}(N_M - 1)(L_{M-M}) \quad (11)$$

$$L_{Cab(Str-Str)} = 2(N_{Str} - 1)(L_{Str-Str}) + 2L_{Inv} \quad (12)$$

By putting L_{M-M} from (5), $L_{Str-Str}$ from (4) and L_{RT} from (8) in to (11) & (12), the L_{Cab_P}

$$L_{Cab(M-M)} = (2N_{str}(N_M - 1) \times W_M \quad (13)$$

$$L_{Cab(Str-Str)} = L_M \times 2(N_{Str} - 1)\left[2Sin(\theta_1) + \frac{Sin(\theta_1)}{Tan(\theta_2)} \right.$$
$$\left. + Cos(\theta_1) + \frac{2H_{G-CL}}{L_M} \right] + (2L_{Inv}) \quad (14)$$

C. SERIES-PARALLEL ARRA

The case of SP interconnection scheme is illustrated in Fig 4. The cable length for module-to-module of every string and for string-to-string of entire array is calculated as $N_{str}(N_M - 1)$ and $2(N_{str} - 1)$, respectively. In SP scheme, the extra cable length in terms of L_{RT} always takes place in addition to $2 \times L_{Inv}$. The final formula for SP is presented as:

$$L_{Cab(M-M)} = N_{str}(N_M - 1)(L_{M-M}) \quad (15)$$

$$L_{Cab(Str-Str)} = 2(N_{str} - 1)(L_{Str-Str}) + (2L_{Inv} + L_{RT}) \quad (16)$$

By putting L_{M-M} from (5), $L_{Str-Str}$ from (4) and L_{RT} from (8) in to (15) & (16) results as:

$$L_{Cab(M-M)} = N_{str}(N_M - 1) \times W_M \quad (17)$$

$$L_{Cab(Str-Str)} = L_M \times 2(N_{str} - 1)\left[2Sin(\theta_1) + \frac{Sin(\theta_1)}{Tan(\theta_2)} \right.$$
$$\left. + Cos(\theta_1) + \frac{2H_{G-CL}}{L_M} \right]$$
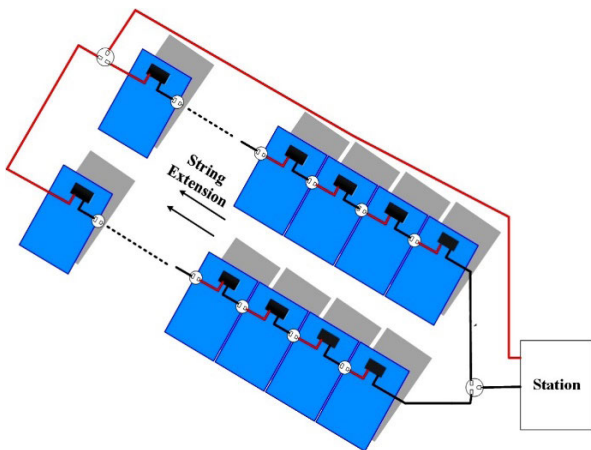$$+ (2L_{Inv} + W_M \times N_{str}) \quad (18)$$

FIGURE 4. Series-parallel connection of Nm × 2 design array.

D. TCT ARRA

The case of TCT interconnection scheme is illustrated in Fig 5. Using module-to-module cable length ($N_{str}(N_M - 1)$) and string-to-string cable length for entire array ($(N_M+1)(N_{str}-1)$), the final formula for TCT is presented as:

$$L_{Cab(M-M)} = N_{str}(N_M - 1)(L_{M-M}) \quad (19)$$

$$L_{Cab(Str-Str)} = (N_M + 1)(N_{str} - 1)(L_{Str-Str})$$
$$+ (2L_{Inv} + L_{RT}) \quad (20)$$

By putting L_{M-M} from (5), $L_{Str-Str}$ from (4) and L_{RT} from (8) in to (19) & (20) results as:

$$L_{Cab(M-M)} = N_{str}(N_M - 1) \times W_M \quad (21)$$

$$L_{Cab(Str-Str)} = L_M \times (N_M + 1)(N_{str} - 1)$$
$$\times \left[2Sin(\theta_1) + \frac{Sin(\theta_1)}{Tan(\theta_2)} + Cos(\theta_1) \right.$$
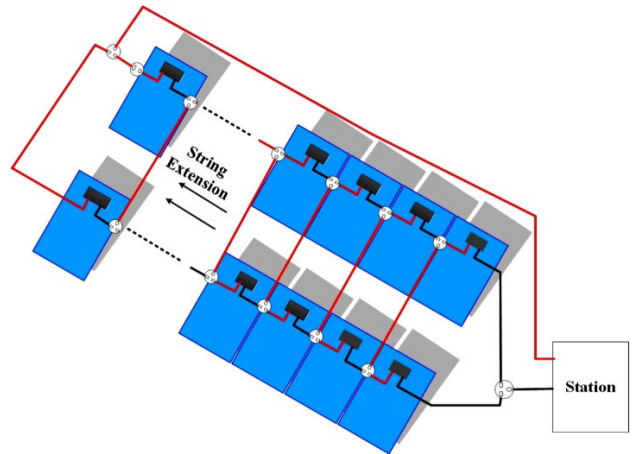$$\left. + \frac{2H_{G-CL}}{L_M} \right] + (2L_{Inv} + W_M \times N_{str}) \quad (22)$$

FIGURE 5. TCT connection of N_m × 2 design array.

E. BL ARRAY

The case of BL interconnection scheme $N_{str}(N_M - 1)$ and $(\frac{N_M}{2}+1)$ respectively represents the cable lengths for module-to-module and string-to-string of entire array. The final formula for BL illustrated in Fig 6 is presented as:

$$L_{Cab(M-M)} = N_{str}(N_M - 1)(L_{M-M}) \quad (23)$$

$$L_{Cab(Str-Str)} = (\frac{N_M}{2} + 1)(N_{str} - 1)(L_{Str-Str})$$
$$+ (2L_{Inv} + L_{RT}) \quad (24)$$

By putting L_{M-M} from (5), $L_{Str-Str}$ from (4) and L_{RT} from (8) in to (23) & (24), results as:

$$L_{Cab(M-M)} = N_{str}(N_M - 1) \times W_M \quad (25)$$

$$L_{Cab(Str-Str)} = L_M \times (\frac{N_M}{2} + 1)(N_{str} - 1)\left[2Sin(\theta_1) \right.$$
$$\left. + \frac{Sin(\theta_1)}{Tan(\theta_2)} + Cos(\theta_1) + \frac{2H_{G-CL}}{L_M} \right]$$
$$+ (2L_{Inv} + W_M \times N_{str}) \quad (26)$$

F. HC ARRAY

The case of HC interconnection scheme with module-to-module cable length ($N_{str}(N_M - 1)$) and string-to-string cable connections of entire array (N_{HC}) is illustrated in Fig 7.
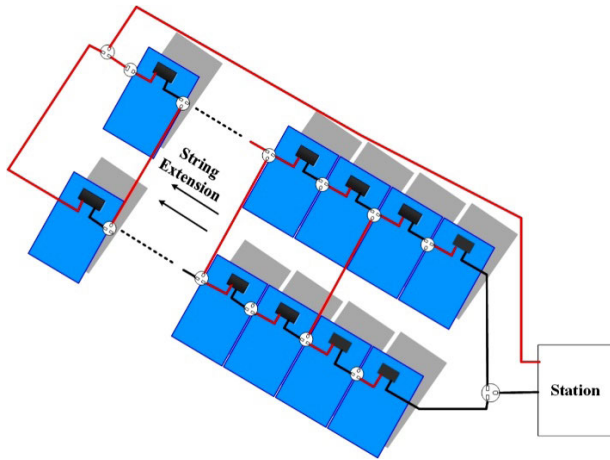
FIGURE 6. BL connection of $N_m \times 2$ design array.

The value of N_{HC} varies depending upon the size of array. The final formula for HC is presented as:

$$L_{Cab(M-M)} = N_{str}(N_M - 1)(L_{M-M}) \qquad (27)$$

$$L_{Cab(Str-Str)} = N_{HC}(L_{Str-Str}) + (2L_{Inv} + L_{RT}) \quad (28)$$

By putting L_{M-M} from (5), $L_{Str-Str}$ from (4) and L_{RT} from (8) in to (27) & (28) results as:

$$L_{Cab(M-M)} = N_{str}(N_M - 1) \times W_M \qquad (29)$$

$$L_{Cab(Str-Str)} = L_M \times (N_{HC}) \left[2Sin(\theta_1) + \frac{Sin(\theta_1)}{Tan(\theta_2)} \right. $$
$$\left. + Cos(\theta_1) + \frac{2H_{G-CL}}{L_M} \right]$$
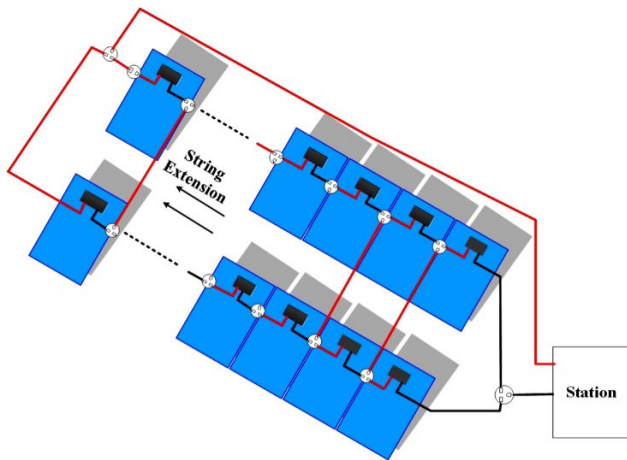$$+ (2L_{Inv} + W_M \times N_{str}) \qquad (30)$$

FIGURE 7. HC connection of $N_m \times 2$ design array.

The aforementioned mathematical modeling of six schemes reveals that with the exception of S scheme, all other schemes are independent of L_{RT} i.e., the cable length for extra round trip. While, the following are the common factors in every scheme:

- No. of modules in an array (N_M)
- No. of strings in an array (N_{str})

- Width of module (W_M)
- Module Tilt angle (θ_1)
- Elevation Angle according to site location (θ_2)
- Length of the cable required to reach the inverter location in station (L_{INV})

III. CRITERION FOR CABLE SELECTION

After calculating the cable length, the cost estimation demands the conductor size of cable in terms of American Wire Gauge (AWG). For this purpose, initially, module-to-module current I_{M_M} and string-to-string current $I_{Str-Str}$ of all interconnection schemes are estimated, which is shown below. The estimations of these currents can be conceptually deduced with the help of pictorial illustrations presented in Fig. 2-7.

S: $I_{M-M} = I_{Str-Str} = I_{sc} \times 1$
P: $I_{M-M} = I_{sc} \times 1$
$I_{Str-Str} = I_{sc} \times N_M$
SP:TCT:BL:HC: $I_{M-M} = I_{sc} \times 1$
$I_{Str-Str} = I_{sc} \times N_{Str}$

The optimum size of DC cable from AWG is selected on the basis of ampacity of the cable, which is determined through three factors:

- Current carrying capacity – The cable should withstand against maximum current without damaging the conductor and insulation.
- Ambient temperature – The insulating material of cable should survive against highest ambient temperature.
- Percentage voltage drop – The resistivity of the conductor should be minimal such that the cable exhibits low voltage drop and therefore, low I^2R losses.

A. CURRENT CARRYING CAPACIT

The estimation of conductor size of the cable is not a trivial task, as it requires several sane assumptions for the PV array [15]. In accordance with standards of NEC 690.8(a)(1) and 690.8(a)(2) [16], the cable should be able to carry 1.56 of I_{sc} of the module as presented in (7). Here, 1.56 is derived from the product of two 1.25 factors: 1) The rated I_{SC} is multiplied by 1.25 to for the ampacity requirements of the cable, interpreted as 125% E ("E" stands for equipment limitation) and 2) An additional factor of 1.25 N ("N" stands for normal operation) is used to account for the module I_{SC} which can be quite above the standard test condition (STC) on an hot and clear day. All established standards like NEC [17], IEC [18], and IEEE [19] are on one page regarding the multiplication factor of 1.56 for PV systems.

$$I_{Rated} = 1.56 \times I_{sc} \qquad (31)$$

B. ADJUSTMENT WITH AMBIENT TEMPERATUR

At elevated temperature and high magnitude of current, heat dissipation from hot cables becomes an issue. For this issue, the temperature correction factor (TCF) is incorporated in I_{Rated} of array as per recommendation of NEC [19], which is presented in (8). To calculate the TCF, firstly, the ambient

temperature (T_A) is needed, which is the sum of the following two temperature factors: Highest temperature (T_H) of the installation field and Temperature (T_o) that accounts for the ground distance between ground surface and conduits containing the DC cable. The value of T_o can be deduced from Table 1 (NEC 310.15(b)(2)(c)) for rooftop PV installation, which revolves around ground distance in mm versus temperature. For the larger ground mounted PV arrays the adjustment factor T_o is usually not applied and will be considered zero because the cable trays are mostly installed behind the PV arrays under shadow. Finally, in accordance with the sum of the two temperature factors i.e., $T_H + T_0$, TCF value is deduced from the Table 2 and I_{Rated} is estimated through (7). Note that TCF is a constant factor with no unit and its value decreases with the increase in the temperature. Section 690.8(b)(1)(c) of the NEC states that TCF shall apply where operating temperatures are greater than 40 °C and if the de-rated ampere is not available then the next highest available rating can be selected.

S:

$$I_{Rated(M-M)} = \frac{1.56 \times I_{M-M}}{TCF} = \frac{1.56 \times I_{sc}}{TCF} \quad (32)$$

$$I_{Rated(Str-Str)} = \frac{1.56 \times I_{Str-Str}}{TCF} = \frac{1.56 \times I_{sc}}{TCF} \quad (33)$$

P:

$$I_{Rated(M-M)} = \frac{1.56 \times I_{M-M}}{TCF} = \frac{1.56 \times I_{sc}}{TCF} \quad (34)$$

$$I_{Rated(Str-Str)} = \frac{1.56 \times I_{Str-Str}}{TCF} = \frac{1.56 \times I_{sc} \times N_M}{TCF} \quad (35)$$

SP, TCT, BL, HC:

$$I_{Rated(M-M)} = \frac{1.56 \times I_{M-M}}{TCF} = \frac{1.56 \times I_{sc}}{TCF} \quad (36)$$

$$I_{Rated(Str-Str)} = \frac{1.56 \times I_{Str-Str}}{TCF} = \frac{1.56 \times I_{sc} \times N_{Str}}{TCF} \quad (37)$$

TABLE 1. Ambient temperature adjustment (w.r.t ground) for conduits exposed to sunlight [17].

Distance between Surface and Conduit	Temperature (T_o) °C
0 – 13 mm (1/2 in.)	33
13 – 90 mm (3.5 in.)	22
90 – 300 mm (12 in.)	17
300 – 900 mm (36 in.)	14

C. VOLTAGE DROP CONSIDERATION

The operating voltage range for the solar inverters is set to be very wide due to the disparity in irradiance levels and ambient temperature. Voltage loss in the cables delivering power to inverters is estimated by traditional rules of thumb. According to which, the maximum voltage drop allowed

TABLE 2. Ambient temperature correction factor [17].

Ambient Temperature (C⁰)	Temperature Correction Factor (TCF)		
	60 C⁰	75 C⁰	90 C⁰
10 or less	1.29	1.20	1.15
11-15	1.22	1.15	1.08
16-20	1.15	1.11	1.08
21-25	1.08	1.05	1.04
26-30	1	1	1
31-35	0.91	0.94	0.96
36-40	0.82	0.88	0.91
41-45	0.71	0.82	0.87
46-50	0.58	0.75	0.82
51-55	0.41	0.67	0.76
56-60	-	0.58	0.71
61-65	-	0.47	0.65
66-70	-	0.33	0.58
71-75	-	-	0.50
76-80	-	-	0.41
81-85	-	-	0.29

in cables for industrial loads is 5% [20]. Such constraint is justified for the loads like motors, computer centers and lighting and other industrial loads affected by voltages lower than their rated value. However, PV inverters can work with a wide range of input voltage i.e., upto 40-50% drop in nominal voltage, the condition of 5% voltage loss in cables can be relaxed. Nevertheless, many designers adopted the 1.5% voltage drop as a standard for losses [20]. In this research work, 1.5% voltage drop (VD) for the total length of each connection type, which are module-to-module and string-to-string connections. Length functions of both are defined in the above section and are used in (21) to estimate Ohm/kilo feet Ω/kft for both connection types. Overall voltage drop will not exceed more than 3% which is less than the 5% commonly used. Table 3 shows that AWG can be selected if temperature rating of conductor and Ω/kft is available. The working temperature ($T_H + TO$) is already estimated during TCF, whileΩ/kft for the total length of connection of module-to-module and string-to-string is estimated from the following expression:

$$\frac{Ohm}{kft}(M-M) = \frac{VD\% \times V_{MPP\_STC}}{I_{Rated(M-M)}} \times \frac{1}{0.1 \times L_{Cab(M-M)}} \quad (38)$$

$$\frac{Ohm}{kft}(Str-Str) = \frac{VD\% \times V_{MPP\_STC}}{I_{Rated(Str-Str)}} \times \frac{1}{0.1 \times L_{Cab(Str-Str)}} \quad (39)$$

$V_{MPP-STC}$ = Array voltage for max power

TABLE 3. AWG selection for cables based on ampacity and operating temperature [19].

Size	Resistance	Cable Ampacity for Different Temperature Rating of Conductor and Insulation Types		
		$60\ C^0$	$75\ C^0$	$90\ C^0$
AWG/kcmil		TYPES (COPPER)		
	$/$	TW, UF	RHW,THHW,THW, THWN,XHHW, USE,ZW	TBS,SA,SIS,FEP,FEPB,MI, RHH, RHW-2, THHN, THHW, THW-2, THWN-2, USE-2,XHH,XHHW,XHHW-2,ZW-2
18	6.385	-	-	14
16	4.016	-	-	18
14	2.525	15	20	25
12	1.588	20	25	30
10	0.998	30	35	40
8	0.628	40	50	55
6	0.395	55	65	75
4	0.248	70	85	95
3	0.197	85	10	115
2	0.156	95	115	130
1/0	0.01	125	150	170
2/0	0.08	145	175	195
3/0	0.062	165	200	225
4/0	0.049	195	230	260

$I_{Rated(M-M)}$ = Rated current of cable connection module-to-module from (32), (34) & (36) depending upon the connection scheme

$I_{Rated(Str-Str)}$ = Rated current of cable connection string-to-string from (33), (35) & (37) depending upon the connection scheme

VD% = Tolerable percentage voltage drop $L_{Cab(M-M)}$ = One-way cabling length in feet from array to the location of inverter station

$\frac{Ohm}{kft}(M-M)$ = cable resistance Ω/kft from (38) for total length of module-to-module connection in whole array

$\frac{Ohm}{kft}$ (Str-Str) = cable resistance Ω/kft from (39) for total length of string-to-string connection in whole array. The value of the Ohm/kft can be found from the NEC table 3 against the selected AWG.

IV. COST ESTIMATION & COMPARATIVE ANALYSIS

The cost estimation of any interconnection scheme requires following steps:

1) Firstly, total lengths of L_{M-M} and $L_{Str-Str}$ is calculated for each scheme.
2) For both $L_{Cab(M-M)}$ and $L_{Cab(Str-Str)}$ lengths calculated in previous step, formula (38) & (39) is invoked to calculate Ohm/kft using Table 3. Thereafter, the standard of DC conductor in terms of AWG standard is selected from Table 3 for L_{M-M} and $L_{Str-Str}$.
3) Cost of AWG in \$/m for both L_{M-M} and $L_{Str-Str}$ is finally multiplied with respective lengths to estimate the overall cabling cost of interconnection scheme. The cost of cable module-to-module ($C_{Cab(M-M)}$) and cost of cable string-to-string ($C_{Cab(Str-Str)}$) will

TABLE 4. Elevation angle of sun of install location for the whole year [15].

MONTH	ELEVATION ANGLE
DEC	11^0
JAN	14^0
FEB	18^0
MAR	25^0
APR	31^0
MAY	36^0
JUN	38^0
AVG. Angle	24.7^0

be different for all array arrangements except series interconnection.

$$C_{M-M} = L_{Cab(M-M)} \times C_{cab(M-M)}(\frac{\$}{m}) \quad (40)$$

$$C_{Str-Str} = L_{Cab(Str-Str)} \times C_{cab(Str-Str)}(\frac{\$}{m}) \quad (41)$$

$$C_{Total} = C_{M-M} + C_{Str-Str} \quad (42)$$

V. DESIGN PROBLEM AND COMPARATIVE STUDY
A. MODULE DIMENSIONS
Model XSSP240P30, V_{mp}, I_{mp}, W_p = 31.8 V, 7.75 A, 240 W
Length of Module = L_M = 1.64 m
Width of Module = W_M = 0.99 m
Open Circuit Voltage (V_{OC}) = 37.5 V
Short Circuit Current (I_{SC}) = 8.49 A

B. ARRAY DIMENSIONS
No. of Modules in one string = N_M = 10
No. of strings = N_{str} = 2
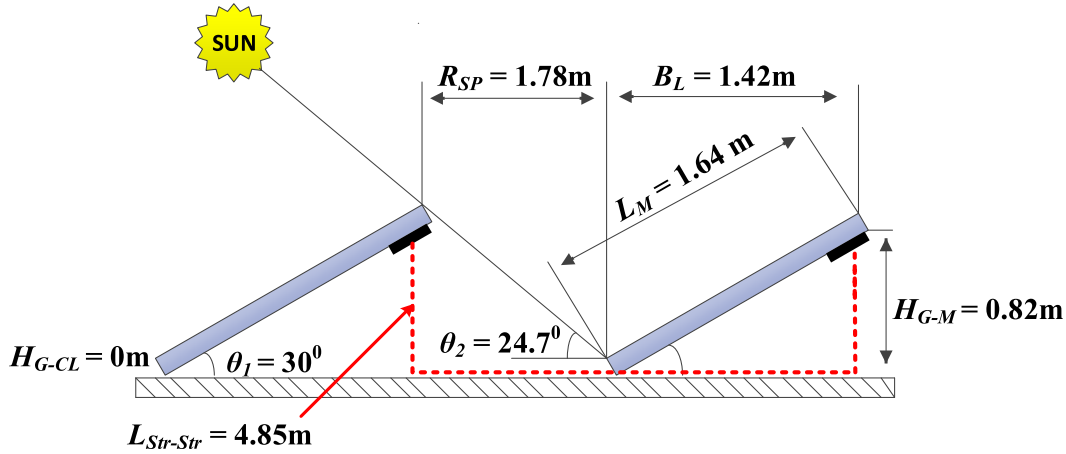Distance of inverter from array location = L_{INV} = 10 m

FIGURE 8. Design values of actual PV array.

C. INSTALLATION LOCATION

Rooftop of University of Central Punjab Lahore Pakistan Longitude & Latitude = 31.4466149 & 74.2679762. On these values of longitude and latitude the estimated values of elevation angle is given in the table below from DEC to JUN. In the duration from JUN to DEC the values of angles keep repeating themselves and average remains unchanged. Tilt angle of the module is 30° for this design example to avoid longer shadows in winter [21].

D. STRINGS SPACING OF PV ARRAY

Using the values of module length, width and tilt angle and elevation angle according to the site location and substituting in (1), (2), (3) & (4), the values of H_{G-M}, R_{SP}, B_L and $L_{Str-Str}$ can be estimated as illustrated in fig 8. H_{G-CL} is considered zero as there is no gap between the lower edge of PV and ground.

Total cabling length can be estimated by using the length function for different array schemes accordingly.

E. AWG SELECTION OF CABLE

Short Circuit Current of Module = I_{SC} = 8.49 A

Highest temp. of installation location = T_H = 45 C°

Ambient Temperature Adjustment = T_o = 33 C° (For 13mm cable distance from ground from Table 1

Design Temperature = $T_H + T_o$ = 78 C°

The ambient temperature could be 78 C° between the roof and the module, so the temperature rating of all terminals, devices, conductors and cables should be 90 C°. The value of TCF = 0.41 can be seen from the table 2 for the design temperature.

F. SERIES ARRAY

Using (9) & (10), $L_{Cab(M-M)}$ = 17.82 m and $L_{Cab(Str-Str)}$ = 24.85 m, current ratings can be estimated using (32) & (33) which are $I_{Rated(M-M)}$ = 32.3A and $I_{Rated(Str-Str)}$ = 32.3A. By substituting the values of $I_{Rated(M-M)}$, $I_{Rated(Str-Str)}$, $L_{Cab(M-M)}$ and $L_{Cab(Str-Str)}$ in (38) & (39) gives the values of resistance/kft for module-to-module and string-to-string

cabling lengths which are $\frac{Ohm}{kft}(M-M)$ = $0.25\frac{\Omega}{kft}$ and $\frac{Ohm}{kft}(Str-Str)$ = $0.185\frac{\Omega}{kft}$. Using these values the appropriate AWG for module-to-module and string –to-string is 4 and 2 respectively selected from table 3. According to NEC (690.31(a)), the PV cables are permitted to be mounted in a cable tray on an outdoor locations, provided the cables are supported at every 300mm and secured at every interval of 1.4m. In this case study ladder and ventilated cable trays are used to protect the cables from falling objects, rodents, water and dust.

Using cable 4 and 3 AWG 1-core, USE-2, bare copper, class 5, finely stranded according to IEC 60228 cl. 5 and the cost given by the manufacturer (METSEC-Cables) is 2.71 $/m and 3.1 $/m respectively. The cable has properties such as: ultra-violet light and weather resistant, abrasion and cut resistant, flame resistant and resistant to short circuit upto 200 °C. Using (40), (41) & (42) the module-to-module (C_{M-M}) and string-to-string ($C_{Str-Str}$) cabling cost is estimated as 48.3$ and 77 $ respectively and the total cabling cost (C_{Total}) for series connection of PV array is 125.4 $.

G. PARALLEL ARRAY

Using (13) & (14), LCab(M-M) = 35.64 m and $L_{Cab(Str-Str)}$ = 29.7 m, current ratings can be estimated using (34) & (35) which are $I_{Rated(M-M)}$ = 32.3A and $I_{Rated(Str-Str)}$ = 323A. By substituting the values of $I_{Rated(M-M)}$, $I_{Rated(Str-Str)}$, $L_{Cab(M-M)}$ and $L_{Cab(Str-Str)}$ in (38) & (39) gives the values of resistance/kft for module-to-module and string-to-string cabling lengths which are $\frac{Ohm}{kft}(M-M)$ = $0.126\frac{\Omega}{kft}$ and $\frac{Ohm}{kft}(Str-Str)$ = $0.015\frac{\Omega}{kft}$. Using these values the appropriate AWG for module-to-module and string-to-string is 2 and 1/0 respectively selected from table 3.

Using cable 2 and 1/0 AWG having cost of 3.71 $/m and 4.98 $/m respectively. Using (40), (41) & (42) the module-to-module (C_{M-M}) and string-to-string ($C_{Str-Str}$) cabling cost is estimated as 132.2 $ and 147.9 $ respectively and the total cabling cost (C_{Total}) for series connection of PV array is 280 $.

TABLE 5. Cost analysis of PV array configurations for the array size 10 × 2.

Configuration Array Size (10×2)	Cable Length		AWG		AWG Cost ($/m)		Total Cost ($)
	$L_{Cab(M-M)}$	$L_{Cab(Str-Str)}$	M-M	Str-Str	M-M	Str-Str	
Series	17.82	24.85	4	3	2.71	3.1	125.3
Parallel	35.64	29.7	2	1/0	3.71	4.98	280
S-P	17.82	26.83	4	2/0	2.71	7.17	275.5
TCT	17.82	75.33	4	4/0	2.71	12.37	980
BL	17.82	51.1	4	4/0	2.71	12.37	680.4
HC	17.82	36.53	4	3/0	2.71	9.84	551.1

H. SERIES-PARALLEL ARRAY

Using (17) & (18), $L_{Cab(M-M)} = 17.82$ m and $L_{Cab(Str-Str)} = 31.68$ m, current ratings can be estimated using (36) & (37) which are $I_{Rated(M-M)} = 32.3$A and $I_{Rated(Str-Str)} = 64.6$A. By substituting the values of $I_{Rated(M-M)}$, $I_{Rated(Str-Str)}$, $L_{Cab(M-M)}$ and $L_{Cab(Str-Str)}$ in (38) & (39) gives the values of Ohm/kft for module-to-module and string-to-string cabling lengths which are $\frac{Ohm}{kft}(M-M) = 0.25\frac{\Omega}{kft}$ and $\frac{Ohm}{kft}(Str-Str) = 0.07\frac{\Omega}{kft}$. Using these values the appropriate AWG for module-to-module and string-to-string is 4 and 2/0 respectively selected from table 3.

Using cable 4 and 2/0 AWG having cost of 2.71 $/m and 7.17 $/m respectively. Using (40), (41) & (42) the module-to-module (C_{M-M}) and string-to-string ($C_{Str-Str}$) cabling cost is estimated as 48.3 $ and 227.1 $ respectively and the total cabling cost (C_{Total}) for series connection of PV array is 275.5 $.

I. TCT ARRAY

Using (21) & (22), $L_{Cab(M-M)} = 17.82$ m and $L_{Cab(Str-Str)} = 75.33$ m, current ratings can be estimated using (36) & (37) which are $I_{Rated(M-M)} = 32.3$A and $I_{Rated(Str-Str)} = 64.6$A. By substituting the values of $I_{Rated(M-M)}$, $I_{Rated(Str-Str)}$, $L_{Cab(M-M)}$ and $L_{Cab(Str-Str)}$ in (38) & (39) gives the values of Ohm/kft for module-to-module and string-to-string cabling lengths which are $\frac{Ohm}{kft}(M-M) = 0.25\frac{\Omega}{kft}$ and $\frac{Ohm}{kft}(Str-Str) = 0.03\frac{\Omega}{kft}$. Using these values the appropriate AWG for module-to-module and string-to-string is 4 and 4/0 respectively selected from table 3.

Using cable 4 and 4/0 AWG having cost of 2.71 $/m and 12.37 $/m respectively. Using (40), (41) & (42) the module-to-module (C_{M-M}) and string-to-string ($C_{Str-Str}$) cabling cost is estimated as 48.3 $ and 931.8 $ respectively and the total cabling cost (C_{Total}) for series connection of PV array is 980 $.

J. BL ARRAY

Using (25) & (26), $L_{Cab(M-M)} = 17.82$ m and $L_{Cab(Str-Str)} = 51.1$ m, current ratings can be estimated using (36) & (37) which are $I_{Rated(M-M)} = 32.3$A and $I_{Rated(Str-Str)} = 64.6$A. By substituting the values of $I_{Rated(M-M)}$, $I_{Rated(Str-Str)}$, $L_{Cab(M-M)}$ and $L_{Cab(Str-Str)}$ in (38) & (39) gives the values of Ohm/kft for module-to-module and string-to-string cabling lengths which are $\frac{Ohm}{kft}(M-M) = 0.25\frac{\Omega}{kft}$ and $\frac{Ohm}{kft}(Str-Str) = 0.044\frac{\Omega}{kft}$. Using these values the appropriate AWG for module-to-module and string-to-string is 4 and 4/0 respectively selected from table 3.

Using cable 4 and 4/0 AWG for the cost of 2.71 $/m and 12.37 $/m respectively. Using (40), (41) & (42) the module-to-module (C_{M-M}) and string-to-string ($C_{Str-Str}$) cabling cost is estimated as 48.3 $ and 632.1 $ respectively and the total cabling cost (C_{Total}) for series connection of PV array is 680.4 $.

K. HC ARRAY

Using (25) & (26), $L_{Cab(M-M)} = 17.82$ m and $L_{Cab(Str-Str)} = 36.53$ m, current ratings can be estimated using (36) & (37) which are $I_{Rated(M-M)} = 32.3$A and $I_{Rated(Str-Str)} = 64.6$A. By substituting the values of $I_{Rated(M-M)}$, $I_{Rated(Str-Str)}$, $L_{Cab(M-M)}$ and $L_{Cab(Str-Str)}$ in (38) & (39) gives the values of Ohm/kft for module-to-module and string-to-string cabling lengths which are $\frac{Ohm}{kft}(M-M) = 0.25\frac{\Omega}{kft}$ and $\frac{Ohm}{kft}(Str-Str) = 0.062\frac{\Omega}{kft}$. Using these values the appropriate AWG for module-to-module and string-to-string is 4 and 3/0 respectively selected from table 3.

Using cable 2 and 3/0 for the cost of 2.71 $/m and 9.84 $/m respectively. Using (40), (41) & (42) the module-to-module (C_{M-M}) and string-to-string ($C_{Str-Str}$) cabling cost is estimated as 48.3 $ and 502.8 $ respectively and the total cabling cost (C_{Total}) for series connection of PV array is 551.1 $.

The comprehensive cost analysis of all six PV array configurations is presented is table 5.

For medium to large scale applications, series and parallel architectures are rarely used. Nevertheless, there are numerous small-scale applications, where two-three panels are connected either in simple series or parallel to form the array such as providing power to highway lights, small mobile-charging station etc. Moreover, there are specific string architectures in which PV array is arranged through dedicated inverter/converter of each string, and each string contains only series connected modules. In this regard, the cost analysis of simple series and parallel architectures is discussed in the paper.

In [22] six different shading patterns are generated to compare the performance of PV configurations under partial shading and TCT is opted as the best as far as the maximum power is concerned under all shading scenarios. Each shade is different from one-another and one can segregate them in the context of horizontal shade, diagonal shade, chess shade, mid-point concentrated shade etc. In connection to these six shades, the overall advantage of one architecture over others gives you a good idea with reasonable certainty. Based on the findings in [22] payback time of the TCT, BL and HC within 10 years is presented in the tables 6-8 taking SP as a benchmark. Percentage additional power of TCT, BL and HC under 5 different shading scenarios is estimated for our design problem using the study in [22]. The highlighted area in the tables depicts events in which the payback time takes more than 10 years to cover the additional cost. Fig 9-11 depict the graphical representation of payback time vs. shading hours over the time span of 10 to 20 years. Fig. 9, 10 & 11 only presents the graphical view of the energy payback time vs. the shading hours, as the increase in number of shading hours tends to decrease the energy payback time. The feasibility and economic viability of each PV plant is estimated with regard to its operation in the MPP region of P-V curve. So, the array is arranged such that inverter will by and large operate the PV array at MPP point. With the help of proposed study, one can see the advantage of one architecture over others and one can arrange the specific architecture in accordance with MPPT setting.

Several photovoltaic technologies are available in the market; crystalline silicon (c-Si) technologies such as mono-Si, poly-Si, and thin-film technologies are widely used commercially. Crystalline Si occupies more than 80% of the market. Nevertheless, thin-film CdTe, because of its stronger temperature coefficient, is getting popular in areas where surface temperatures are reasonably higher [23]. With respect to the loss of performance and degradation of existing technologies, the c-Si and thin-film modules are evaluated in [24]. It is revealed that the average yearly efficiency decreases from 14% to 11% for c-Si module having an efficiency of 14.75% at STC. While, the decaying rate of efficiency is 8% to 6% for thin film modules with 9.15% efficiency at STC. Annual degradation rates of thin film modules and c-Si modules are considered to be 1.3%/year and 1.6%/year, respectively.

TABLE 6. Payback time vs No. of shading Hours per day for TCT in 10 years.

Configuration Array Size (10×2)	4800 (W)	Shading Hours/Day			
Add. Power (TCT)	Add. Cost ($)	1	2	3	Pay Back Time (Years)
3%	144		67.1	33.5	22.4	
5%	240		40.2	20.1	13.4	
10%	480	705	20.1	10.1	6.7	
15%	720		13.4	6.7	4.5	
20%	960		10.1	5	3.4	

TABLE 7. Payback time vs No. of shading Hours per day for BL in 10 years.

Configuration Array Size (10×2)	4800 (W)	Shading Hours/Day			
Add. Power (BL)	Add. Cost ($)	1	2	3	Pay Back Time (Years)
0.5%	24		231.2	115.6	77.1	
1%	48		115.6	57.8	38.5	
2%	96	405	57.8	28.9	19.3	
3%	144		38.5	19.3	12.8	
4%	182		28.9	14.4	9.6	

TABLE 8. Payback time vs. No. of shading Hours per day for HC in 10 years.

Configuration Array Size (10×2)	4800 (W)	Shading Hours/Day			
Add. Power (HC)	Add. Cost ($)	1	2	3	Pay Back Time (Years)
0.3%	14.4		262.6	131.3	87.5	
1.5%	72		52.5	26.3	17.5	
2.5%	120	276	31.5	15.8	10.5	
3%	144		26.3	13.1	8.8	
4%	192		17.9	9.8	6.6	

In [25] the costs related with c-Si and thin-film modules are analyzed, with saving potential of up to 0.04 $/W, 0.10 $/W, and 0.13 $/W in module production costs for c-Si, CdTe, and CIGS respectively, with large area modules. Note that these savings depend on the ability to maintain efficiency and production output. However, in these studies, the factor of cabling cost is a missing link.
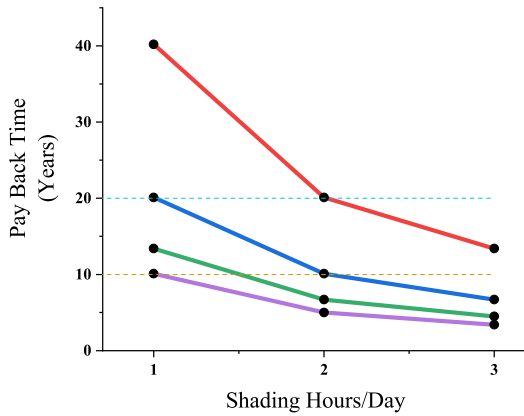
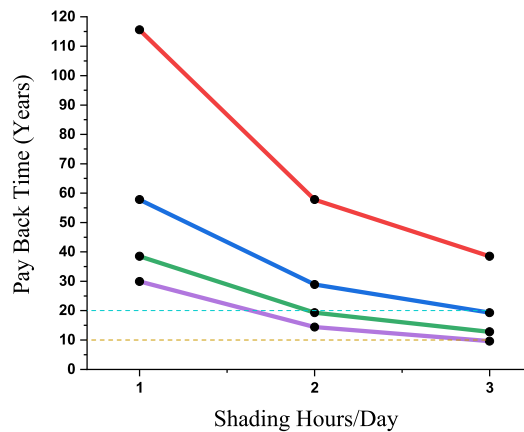**FIGURE 9.** Payback time Vs. No. of shading Hours per day for TCT.

FIGURE 10. Payback time Vs. No. of shading Hours per day for BL.
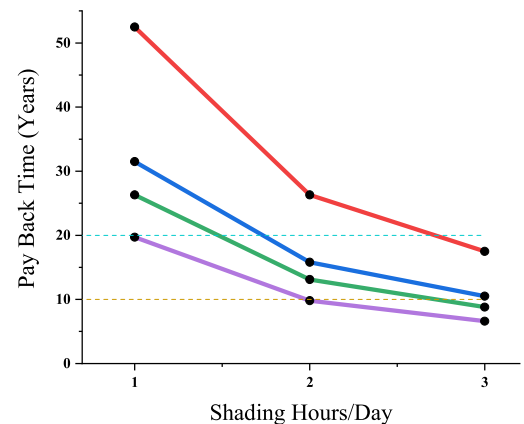

FIGURE 11. Payback time vs. no. of shading Hours per day for HC.

This research work incorporates the cabling constraint and discusses the energy payback time of six PV architectures using c-Si modules. Nevertheless, by following the footprints of the proposed method, the payback time of other technology such as thin-film module based PV plant can be estimated.

VI. CONCLUDING REMARKS
In this article cost analysis of different PV array configurations is presented for different array sizes. Analysis consist of

two steps, in the 1st step proper AWG of the cable is selected based on ampacity and temperature requirements. In the 2nd step cable length is estimated required for different PV array configurations such as Series-Parallel (S-P), Total-cross-tied (TCT), Bridge-Link (BL) and Honey-Comb (HC). At the end a design problem is presented for a 10×2 size array, giving the estimated cost for all possible configurations.

For all the configurations TCT cabling cost is the highest among due to several inter strings connections followed by HC and BL. Considering the advantage of less power loss for TCT and HC under partial shading, there is a disadvantage of higher cost of implementation. Percentage additional power of TCT, BL and HC under 5 different shading scenarios is estimated taking SP as a benchmark and the highlighted area in the tables depicts events in which the payback time takes more than 10 years to cover the additional cost. In most of the scenarios the payback time is exceeding the life limit of PV cell operating at maximum efficiency. The cost analysis provides a clear snapshot for energy payback time of each architecture, which is a missing link in the literature. The results clearly depicts that on the ground of minimum energy payback time SP is the optimal choice, when compared with the other interconnection PV array architectures.

REFERENCES
[1] R. Pachauri, R. Singh, A. Gehlot, R. Samakaria, and S. Choudhury, "Experimental analysis to extract maximum power from PV array reconfiguration under partial shading conditions," *Eng. Sci. Technol., Int. J.*, vol. 22, no. 1, pp. 109–130, Feb. 2019.
[2] L. El Lysaouy, "Anoval magic square view topology of PV under partial shading," *Energy Procedia*, vol. 157, pp. 1182–1190, May 2019.
[3] E. I. Lahcen, "Enhancing the performances of PV array configurations under partially shaded conditions: A comparative study," *Int. J. Renew. Energy Res.*, vol. 8, no. 3, p. 151, 2018.
[4] S. R. Pendem and S. Mikkili, "Modeling, simulation and performance analysis of solar PV array configurations (series, series–Parallel and honey-Comb) to extract maximum power under partial shading conditions," *Energy Rep.*, vol. 4, pp. 274–287, Nov. 2018.
[5] P. V. Deshpande1 and B. S. Bodkhe, "Analysis of various connection configuration of photovoltaic module under different shading conditions," *Int. J. Appl. Eng. Res.*, vol. 12, no. 16, pp. 5715–5720, 2017.
[6] P. Srinivasa Rao, G. Saravana Ilango, and C. Nagamani, "Maximum power from PV arrays using a fixed configuration under different shading conditions," *IEEE J. Photovolt.*, vol. 4, no. 2, pp. 679–686, Mar. 2014.
[7] M. K. Alam, F. Khan, J. Johnson, and J. Flicker, "A comprehensive review of catastrophic faults in PV arrays: Types, detection, and mitigation techniques," *IEEE J. Photovolt.*, vol. 5, no. 3, pp. 982–997, May 2015.
[8] B. I. Rani, G. S. Ilango, and C. Nagamani, "Enhanced power generation from PV array under partial shading conditions by shade dispersion using su do ku configuration," *IEEE Trans. Sustain. Energy*, vol. 4, no. 3, pp. 594–601, Jul. 2013.
[9] K.-N.-D. Malamaki and C. S. Demoulias, "Minimization of electrical losses in two-axis tracking PV systems," *IEEE Trans. Power Del.*, vol. 28, no. 4, pp. 2445–2455, Oct. 2013.
[10] R. Ramaprabha and B. L. Mathur, "A comprehensive review and analysis of solar photovoltaic array configurations under partial shaded conditions," *Int. J. Photoenergy*, vol. 2012, pp. 1–16, Dec. 2012, doi: 10.1155/2012/120214.
[11] G. Velasco-Quesada, F. Guinjoan-Gispert, R. Pique-Lopez, M. Roman-Lumbreras, and A. Conesa-Roca, "Electrical PV array reconfiguration strategy for energy extraction improvement in grid-connected PV systems," *IEEE Trans. Ind. Electron.*, vol. 56, no. 11, pp. 4319–4331, Nov. 2009.
[12] H. Ziar, S. Farhangi, and B. Asaei, "Modification to wiring and protection standards of photovoltaic systems," *IEEE J. Photovolt.*, vol. 4, no. 6, pp. 1603–1609, Nov. 2014.

[13] M. J. de Wild-Scholten and E. A. Alsema, "A cost and environmental impact comparison of grid-connected rooftop and ground-based PV systems," in *Proc. 21th Eur. Photovoltaic Solar Energy Conf.*, Dresden, Germany, Sep. 2006, pp. 4–8.

[14] A. Richter, M. Hermle, and S. W. Glunz, "Reassessment of the limiting efficiency for crystalline silicon solar cells," *IEEE J. Photovolt.*, vol. 3, no. 4, pp. 1184–1191, Oct. 2013.

[15] *University of Oregon Solar Radiation Monitoring Laboratory*. Accessed: Nov. 15, 2019. [Online]. Available: http://solardat.uoregon.edu/SunChartProgram.php

[16] (2018). *Pak Cables Manufactures Price Catalog*. [Online]. Available: www.pakistancables.com/media/20692/retail02jul2018.pdf

[17] *National Electrical Code, Article 690-Solar Photovoltaic Systems*, NFPA, Quincy, MA, USA, 2011.

[18] *Electrical Installations of Buildings-Part7-712: Requirements for Special Installations or Locations-Solar Photovoltaic Power Supply Systems*, document IEC 60364-7-712, 2002.

[19] (2018). *Photovoltaic Power Systems and the National Electrical Code*. [Online]. Available: http://www.nmsu.edu/~tdi/Photovoltaics/Codes-Stds/PVnecSugPract.html

[20] P. Andersson and P. Van Hees, "Performance of cables subject to thermal radiation," Swedish Nat. Test. Res. Inst., Borås, Sweden, SP Rep. 2000:24, 2000.

[21] *Don Mulvey Executive Vice President Design Considerations for DC Wiring*. Accessed: Nov. 20, 2019. [Online]. Available: http://www.roallivingenergy.com

[22] O. Bingöl and B. Özkaya, "Analysis and comparison of different PV array configurations under partial shading conditions," *Sol. Energy*, vol. 160, pp. 336–343, Jan. 2018.

[23] A. H. Munshi, N. Sasidharan, S. Pinkayan, K. L. Barth, W. S. Sampath, and W. Ongsakul, "Thin-film CdTe photovoltaics—The technology for utility scale sustainable energy generation," *Sol. Energy*, vol. 173, pp. 511–516, Oct. 2018.

[24] T. Ozden, B. G. Akinoglu, and S. Kurtz, "Performance and degradation analyses of two different PV modules in central Anatolia," in *Proc. Int. Conf. Photovolt. Sci. Technol. (PVCon)*, Ankara, Turkey, Jul. 2018, doi: 10.1109/PVCon.2018.8523880.

[25] K. Horowitz, R. Fu, T. Silverman, M. Woodhouse, X. Sun, and M. Alam, "An analysis of the cost and performance of photovoltaic systems as a function of module area," Tech. Rep., 2017.

[26] *IEEE Guide for Terrestrial Photovoltaic Power System Safety*, Standard 1374, Sep. 1998.

FAHAD USMAN KHAN received the B.Sc. and M.Sc. degrees from the University of Engineering and Technology at Taxila, Taxila, Pakistan. He is currently working as a Lecturer at the Faculty of Engineering, University of Central Punjab (UCP), Lahore, Pakistan. At UCP, he is a member of an active research group (Efficient Electrical Energy Systems). His research interests include the design of solar PV converters and IV curve tracing. He is the author/coauthor of more than two publications.

ALI FAISAL MURTAZA (Member, IEEE) received the B.Sc. degree from the National University of Sciences and Technology (NUST), Rawalpindi, Pakistan, the M.Sc. degree from the University of Engineering and Technology (UET), Lahore, Pakistan, and the Ph.D. degree from the Politecnico di Torino, Turin, Italy. He is currently working as a Director Research and Associate Professor at the Faculty of Engineering, University of Central Punjab (UCP), Lahore. At UCP, a research group (Efficient Electrical Energy Systems) is active under his supervision. His research interests include the design of solar photovoltaic (PV) systems, including dc micro-grids, dc–dc converters, I–V curve tracing, maximum power point trackers, and partial shading effects. He is the author/coauthor of more than 35 publications.
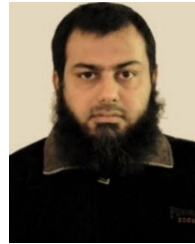
HADEED AHMED SHER (Senior Member, IEEE) received the B.Sc. degree from Bahauddin Zakariya University, Multan, Pakistan, in 2005, the M.Sc. degree from the University of Engineering and Technology at Lahore, Lahore, Pakistan, in 2008, and the Ph.D. degree from King Saud University (KSU), Riyadh, Saudi Arabia, in 2016, all in electrical engineering. He is currently an Assistant Professor with the Faculty of Electrical Engineering, Ghulam Ishaq Khan Institute of Engineering Sciences and Technology, Topi, Pakistan. His current research interests include grid connected solar photovoltaic systems, maximum power point tracking, and power electronics. He received the Research Excellence Award from the KSU College of Engineering, for the year 2012 and 2015.

KAMAL AL-HADDAD (Life Fellow, IEEE) received the B.Sc. and M.Sc. degrees from the Université du Québec à Trois-Rivières, Canada, in 1982 and 1984, respectively, and the Ph.D. degree from the Institut National Polytechnique de Toulouse, Toulouse, France, in 1988. Since June 1990, he has been a Professor with the Electrical Engineering Department, École de Technologie Supérieure (ETS), Montreal, QC, Canada, where he has been the holder of the Senior Canada Research Chair in Electric Energy Conversion and Power Electronics, since 2002. He has supervised more than 170 Ph.D. and M.Sc. students working in the field of power electronics. He is a Consultant and has established very solid link with many Canadian industries working in the field of power electronics, electric transportation, aeronautics, and telecommunications. He has coauthored more than 600 transactions and conference papers. His research interests include high-efficient static power converters, harmonics and reactive power control using hybrid filters, switch mode, resonant, and multilevel converters, including the modeling, control, and development of prototypes for various industrial applications in electric traction, renewable energy, power supplies for drives, telecommunications, and so on. He is a Fellow Member of The Canadian Academy of Engineering, a member of the Academy of Sciences, and a Fellow of The Royal Society of Canada. He was a recipient of the 2014 IEEE IES Dr.-Ing. Eugene Mittelmann Achievement Award. He is the IEEE IES President, from 2016 to 2017, an Associate Editor of the IEEE TRANSACTIONS ON INDUSTRIAL INFORMATICS, and an IES Distinguished Lecturer.

FAISAL MUSTAFA received the Ph.D. degree from the University of Huddersfield, U.K. He has 18 years' international career as a Professor, a Data Scientist, a Senior BI Consultant, an IT Transformation Director, and a Lead Researcher. He brings with him an excellent higher education academic, industrial collaboration, and administrative record. His research interests include business information system development, business intelligence, business forecasting, business simulation modeling, investment valuation and analysis, artificial intelligence, AI planning, advanced business innovations, and semantic web services platform for businesses. His academia action research strand focuses on multidisciplinary curriculum development, inclusive learning and participatory engagement in a collaborative research environment to support teaching and learning in lifelong sector. He is the author/coauthor of more than 20 publications.

● ● ●